WIND AND WAVE DATA ANALYSIS FOR THE LEBANESE COASTAL AREA-PRELIMINARY RESULTS

N. Kabbara
National Council for Scientific Research, National Center for Marine Sciences, Beirut, Lebanon
nkabbara@cnrs.edu.lb

(Received 11 October 2004 - Accepted 23 August 2005)

ABSTRACT

In this paper, a statistical analysis on wind and wave data measurements obtained during a two-year period (2000-2003) is presented. Measurements are produced by the Lebanon Meteorological Network of the Ministry of Public Work and Transport operated by the Department of Meteorology at Beirut Airport. Although the two-year period is short for a statistical descriptive analysis of the local wind and wave climate, the obtained results presented in this paper reveal the general characteristics of wind and wave climate in the study area.

Keywords: wave data analysis, wave climate, wind data analysis, Lebanese coastal area

INTRODUCTION

The Department of Meteorology of the Ministry of Public Work and Transport, Lebanon, uses a monitoring network of eleven meteorological stations distributed all over Lebanon, six of them are on-shore, providing information concerning wind speed and direction, air temperature, relative humidity, and atmospheric pressure, in the form of time series for at least the last 20 years, and three wave buoys located in El-Baddawi north of Tripoli (north of Lebanon), Beirut, and El-Zahrani (south of Lebanon) providing information about wave parameters and sea surface temperature. These data are systematically collected for the last five years and provided by the department of Meteorology at Beirut airport, but for some years the existing wave data are sparse and the measurement period extends only to some months. The meteorological monitoring network is used mainly for navigation, climatologic and other purposes (Beirut Airport), and a wave monitoring system for ship routing and port management. On the other hand, satellite wave data for the Levantine Basin are available as altimetry products from the ERS-2 (repeat period 35 days), and Geosat Follow On- GFO (repeat period 17 days) satellite missions (Krogstad & Barstow, 1999; EuroGOOS Space Panel, 2001). Different wave models are used to forecast the wave climate in the Mediterranean Sea. All global and regional wave forecasts use the UNIWAVE spectral wave model (Cardone *et al*., 1996). This model can be applied with second generation (2G, ODGP-2) or third generation (3G, OWI3G) physics (Khandekar *et al*., 1994) and in either deep water or shallow water mode. Since 1994, wave output at analysis time has been displayed on OWI's web site (www.oceanweather.com) for general use of the maritime community. For the Northwest area of the Levantine Basin, POSEIDON weather forecasting

system, operated by the Institute of Oceanography of the National Center for Marine Research in Greece, uses the wave forecasting model WAM cycle-4 to give model forecasts for wave climate in the Aegean Sea (Christopoulos & Koutitas, 1991; Chritopoulos *et al*., 2000). A detailed description of the POSEIDON system is given by Soukissian *et al*. (1999). A systematic comparison of WAM results with results of DAUT and MIKE 21 OSW, version 2.7 (wave model developed by the Danish Hydraulic Institute) is given by Soukissian *et al*. (2001).

The aim of this paper is to perform a preliminary statistical analysis of two-year (2000-2003) measured wind and wave data at two near-shore locations for the Lebanese coastal area (Figure 1):

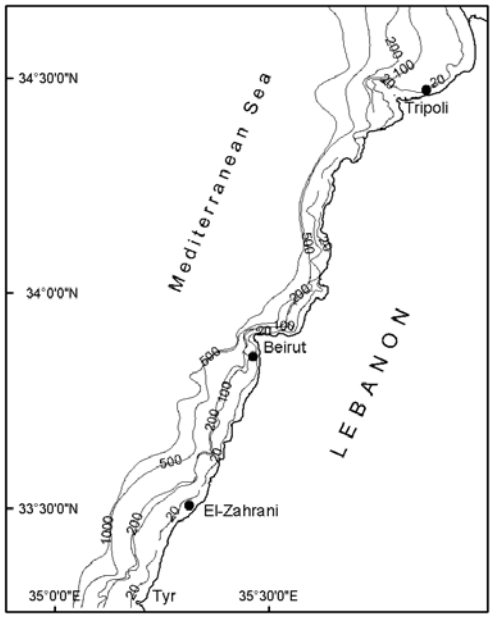

Figure 1. Buoy locations in the Lebanese coastal water.

- Location 1: Beirut-Golf, South of Beirut (Beirut-Golf wave buoy and Beirut Airport meteorological station, 33° 50' 866" N- 35° 28' 516" E),
- Location 2: El-Baddawi, North of Tripoli, (El-Baddawi wave buoy and meteorological station, 34° 28' N - 35° 52' 30" E).

El-Zahrani wave buoy is still not operational.

The most important measured wave parameters are:

- The spectral significant wave height H_{m0}

$$H_{m0} = 4\sqrt{m_0}$$

Where m_n , n = 0, 1, 2, … represent the nth-order moment of the spectral density function $S_{nn}(\omega)$ of the sea surface elevation. (The lower and upper frequencies for the spectral moment calculations are ω_0 = 0.04 Hz and ω_1 = 0.49 Hz, respectively

- The mean zero up-crossing period T_{02}

$$T_{02} = \sqrt{\frac{m_0}{m_2}}$$

- The mean wave direction Θ_W

$$\Theta_W = \arctan\left(\frac{b}{a}\right)$$

where

$$a = \frac{\int_{\omega_0}^{\omega_1} S_{nn}(\omega)\cos\varphi(\omega)d\omega}{m_0}, \; b = \frac{\int_{\omega_0}^{\omega_1} S_{nn}(\omega)\sin\varphi(\omega)d\omega}{m_0}$$

and $\varphi(\omega)$ is the (frequency dependent) wave direction.

The directional wave parameters are obtained by an ordinary directional wave analysis (performed on the CPU of buoys), the recording interval of the wave measurements is 1 h with a sampling period of 20 min. The measured wind parameters are the wind speed u_w , and the mean wind direction θ_w . The recording interval of the wind measurements is 1 h with a sampling period of 10 min. All the above recording and sampling periods are user-selectable. In (Soukissian & Theochari, 2001) it was shown that the basic statistics of the population of the most important wave and wind parameters remain almost the same independently of the recording interval used through the measurements (for recording intervals from 1 up to 5 h).

The total length of the shoreline of Lebanon is 225 Km. The continental shelf off Lebanon is widest in its northern part located between Enfa (near Batroun) and the Syrian borders. In this area it attains a width of 18 Km. Here; the coast has expanses of sandy beaches, and few rocky headlands. Southward, between Enfa and Ras Beirut, the shelf narrows to less than 3 Km. The coast is rocky, with cliffs, very few bays and almost no sandy beaches. South of Ras Beirut, towards Tyre and the southern borders, the shelf widens again

to attain a width 6-7 Km. In this area the coast has many bays and long sandy beaches separated by a few rocky promontories. The upper part of the continental shelf is interrupted by a series of deep submarine canyons (Goedicke, 1972).

ANALYSIS OF WIND AND WAVE MEASUREMENTS

The main statistical characteristics of the available two-year population of wind and wave measurements for each of the two locations are summarized in Table 1. More specifically, the population size, *N*, the mean values μ_H, μ_T and μ_{U_W}, and standard deviations σ_H, σ_T and σ_{U_W} of H_{m0}, T_{02} and u_w, respectively, are presented.

TABLE 1

Descriptive Statistics of Measured Wind and Wave Data during 2000-2003

	Location1	Location2
N	14034	8057
$\mu_H(m)$	0.70	0.36
$\sigma_H(m)$	0.52	0.24
$\mu_T(s)$	4.21	3.35
$\sigma_T(s)$	1.23	1.06
μ_{U_W} $(nots)$	4.68	6.70
$\sigma_{U_W}(nots)$	3.06	5.75

The time series of $H_{m0}(t)$, $T_{02}(t)$, and $u_w(t)$ for the two locations exhibit an apparent seasonality and an annual periodicity. Based on the two-year time series, the mean monthly values of u_w and H_{m0} are calculated and their fluctuation is presented in Figures 2-3.

The months revealing the most intense -in the mean- wind and wave conditions, as can be seen from the Figures 2-3, are presented in Table II. It is clear from these figures that the mean monthly wave period, wave height, and wind speed variation follow similar behaviour.

A wave storm analysis during the measurement period resulted in the two most severe wave storms, occurred at Beirut-Golf. The most severe storm for Beirut-Golf occurred in January 2000. For a threshold level H_{m0} =2m, the storm duration $\Delta\tau$ was 55 h (*i.e.* during that period $H_{m0} \geq$ 2m) and the highly fluctuating wind speed was measured from 3 knots to $u_{W,\max} = 20$ knots. The $H_{m0} >$ 3 m –sea state persisted for 43 h, whilst the maximum wave height and wind gust recorded were $H_{m0,\max} = 8.81$ m and $u_{Gust,\max} = 25$ knots respectively. The most severe storm for Tripoli occurred in March 2000. For a threshold level

H_{m0} =1.5 m, the storm duration $\Delta\tau$ was 14 h and the highly fluctuating wind speed was measured from 8 knots to 23 knots. The maximum wave height and wind gust recorded were $H_{m0,\max} = 1.8$ m and $u_{Gust,\max} = 31$ knots respectively. It is to be noted that during the storm generation and propagation the correlation between the wind speed and the significant wave height is r_{HT} =0.78 without lag.

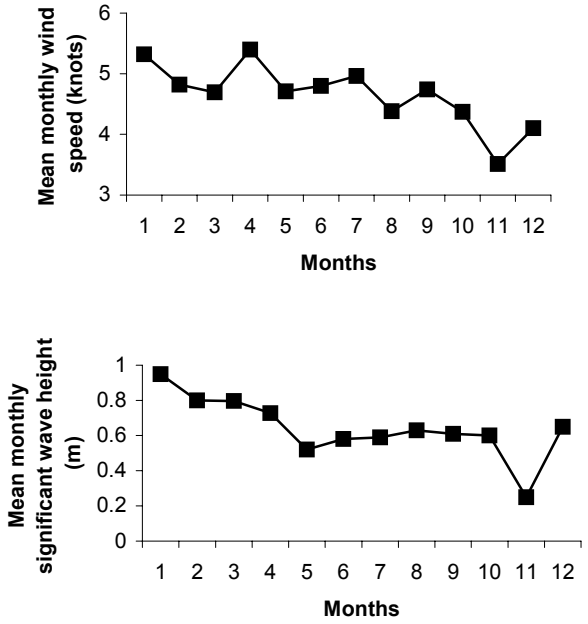

Figure 2. Time series of mean monthly wind speed and significant wave height as obtained from measurements for location 1.

TABLE 2

Months Characterized by the Most Intense –in the Mean- Wind and Wave Conditions

	Location 1	Location 2
Wind speed	January April	January September
Wave height	January February	January February

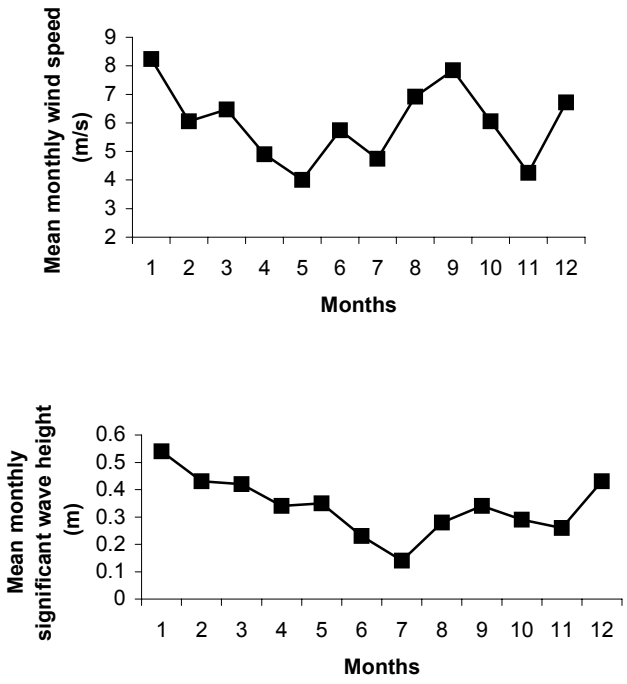

Figure 3. Time series of mean monthly wind speed and significant wave height as obtained from measurements for location 2.

Figures 4-5 give the annual histograms of wind speed u_w from measurements for locations 1 and 2 and Figures 6-7 give the annual histograms of significant wave height H_{m0} from measurements for locations 1 and 2. The scatter diagrams of Figures 8-9 give the relation between the significant wave height H_{m0} and the mean zero up-crossing periods T_{02} for the two locations. For the two locations there is a fair correlation between H_{m0} and T_{02}: For location 1, the correlation coefficient takes a maximum value equal to r_{HT} = 0.52 for a time lag between wind speed and significant wave height equal to 4 hours, while for location 2 it has a maximum value r_{HT} = 0.62 for a time lag equal to 2 hours only. Furthermore, the breaking limit curve $H_{m0} = f(T_{02})$ for the two locations can be easily identified. It is to be noted that for location 2 very low wave height (of about 0.1-0.4 m) is associated to an unexpectedly high wave period (from about 4.5-7.5 s). Since waves with such characteristics can hardly be wind or swell waves, a possible explanation is that such waves are generated by ship traffic, the wave period and height depending mainly on the ship speed and size and the bottom topography.

Figure 4. Annual histogram of wind speed u_w from measurements for location 1.

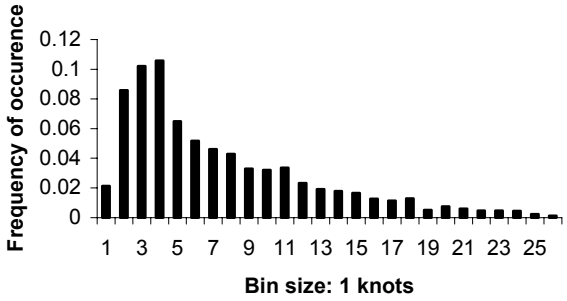

Figure 5. Annual histogram of wind speed u_w from measurements for location 2.

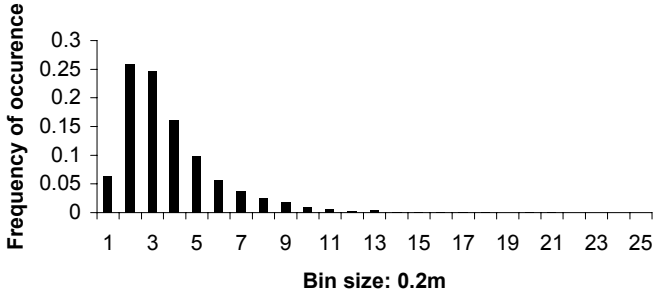

Figure 6. Annual histogram of significant wave height H_{m0} from measurements for location 1.

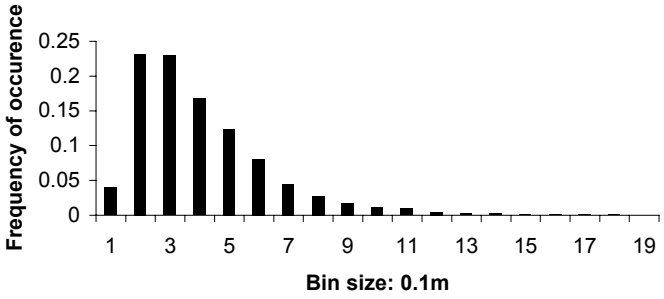

Figure 7. Annual histogram of significant wave height H_{m0} from measurements for location 2.

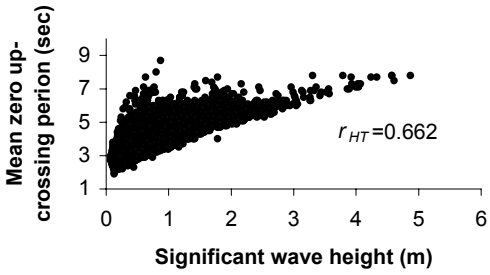

Figure 8. Scatter diagram of measured significant wave height H_{m0} *vs.* mean zero up crossing period T_{02} for location 1.

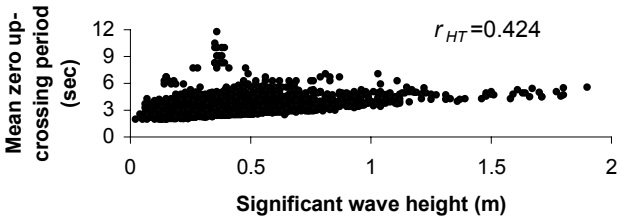

Figure 9. Scatter diagram of measured significant wave height H_{m0} *vs.* mean zero up crossing period T_{02} for location 1.

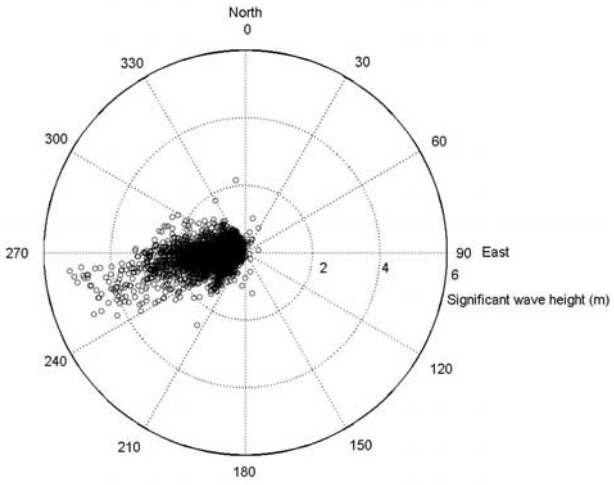

Figure 10. Polar scatter diagram of measured significant wave height H_{m0} *vs.* mean wave direction Θ_w for location Beirut.

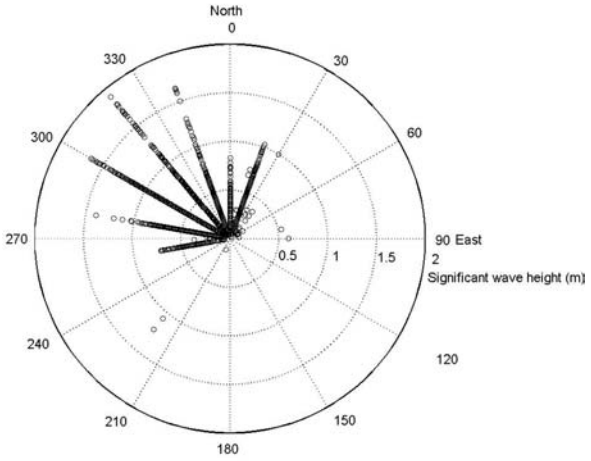

Figure 11. Polar scatter diagram of measured significant wave height H_{m0} *vs.* mean wave direction Θ_w for location Tripoli.

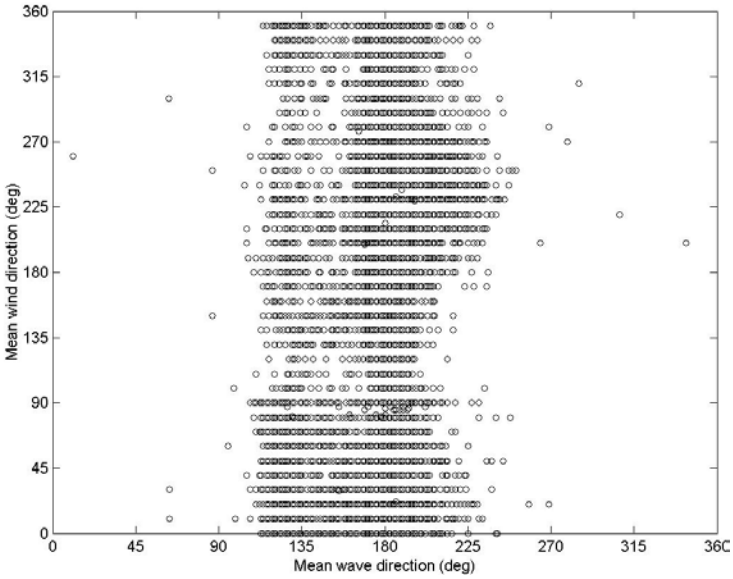

Figure 12. Scatter diagram of measured mean wave direction Θ_w *vs.* mean wind direction θ_w for location 1.

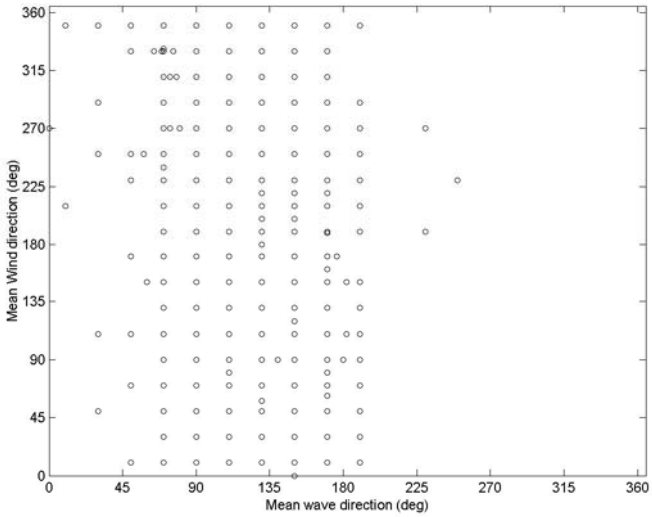

Figure 13. Scatter diagram of measured mean wave direction Θ_w *vs.* mean wind direction θ_w for location 2.

The directional distribution of the significant wave height H_{m0} for locations 1-2 is depicted on the polar scatter diagrams of H_{m0} with respect to the mean wave direction Θ_W (Figures 10-11). The relation of the mean wave direction Θ_W to the wind direction θ_w for both locations can be assessed through the corresponding scatter diagrams shown in Figures 12-13. For location 1 the waves propagate mostly from the W-SW sector 210°-300° (Figure 10). The highest recorded waves ($H_{m0} > 3$ m) propagate from the sector 240°-270° (in this case H_{m0} and Θ_W are fairly linear related). For location 2 waves mainly propagate from the sector 270° to 360°.The wind directions corresponding to the remaining wave directions for both locations (Figures 12-13) are rather scattered indicating an influence of swell waves. For location 1 the angle between the wave crest and the shoreline generally was open to the north. This means that the wave-induced longshore current should have been directed along the coast to the north-northeast. Aerial photographs provide information regarding the direction of longshore transport of beach sand. They show that the mouth of Nahr el Ghadir was deflected to the north as were the Nahr Beirut and Nahr el Kelb along with their discharges of turbid water reached several hundred meters offshore. Such a longshore current agrees with the evidence provided by large accumulations of sand as dunes just south of the coastal projections at Beirut. For location 2 the wave-induced longshore current should have been dominantly directed along the coast to the northeast. Many coastal constructions, especially south of Beirut, were destroyed repeatedly by storm waves during the winter, resulting in increased erosion of the land and loss of sand and accordingly precautions should be taken to preserve the shoreline and existing sand beaches.

CONCLUSION

This paper presents the results of statistical analysis of wind and wave measurement data obtained from two wave buoys: Beirut-Golf (south of Beirut) and El-Baddawi (north of Tripoli) for the two-year period 2000-2003. The results of analysis can be summarized as follows: The most intense period as regards the wave and wind conditions in the Lebanese coastal area extends from November to March. The maximum wave height recorded during this period was 9 m and occurred in Beirut-Golf (south of Beirut). For Tripoli area, very low wave height is associated to an unexpectedly high wave period. These waves can be generated only by ship traffic. The influence of swell waves is evident in both locations Beirut and Tripoli.

ACKNOWLEDGEMENT

Appreciation is due to Mr. Abdo Bajjani and Mr. Riad Assolh Al-Khodari, at the Ministry of Transport, Beirut Airport, Meteorological Division, for their help in acquiring wave and wind measurement data.

REFERENCES

Cardone, V.J., Jensen, R.E., Resio, D.T., Swail, V.R. and Cox, A.T. 1996. Evaluation of contemporary ocean wave models in rare extreme events: Halloween storm of October, 1991; Storm of the century of March, 1993. *J. of Atmos. and Ocean. Tech.*, 13: 198-230.

Christopoulos, S. & Koutitas, C. 1991. Wave modelling in the North Aegean Sea. *Ann. Geophysicae*, 9: 91-101.

Christopoulos, S., Koutitas, C., Soukissian, T.H. and Prevoliotis, L. 2000. Numerical results of the DAUT wave forecasting model in the context of the POSEIDON project (in Greek). *Proceedings of the 16th Symposium on Oceanography and Fisheries*, 1: 407-411, Chios, May.

EuroGOOS Space Panel. 2001. Font, J., Guymer, T.H., Johanessen, J., Van der Kolff, G. H., le Provost, C., Ratier, A., Williams, D. and Flemming, N. C. Operational ocean observations from space. *EuroGOOS Publication No. 16*, Report of the EuroGOOS Conference on Operational Ocean Observations from Space, Darmstadt, Germany.

Goedicke, T.R. 1972. Submarine canyons on the central continental shelf of Lebanon. pp.655-670, in: *The Mediterranean Sea: A natural sedimentation laboratory*. D.J. Stanley ed., Dowden, Hutchinson & Ross Inc., Stroudsburg, Pa., 765pp.

Khandekar, M.L., Lalbeharry, R. & Cardone, V.J. 1994. The performance of the Canadian Spectral Ocean Wave Model (CSOWM) During the Grand Banks ERS-1 SAR Wave Spectral Validation Experiment. *Atmosphere-Ocean* 31 (1): 31-60.

Krogstad, H. E. & Barstow, S. F. 1999. Satellite wave measurements for coastal engineering applications. *Coastal Engineering*, 37: 283-307.

Soukissian, T.H., Chronis, G. Th. and Nittis, K. 1999. "POSEIDON: operational marine monitoring system for Greek seas. *Sea Technology*, 40(7): 32-37.

Soukissian, T., Perivoliotis, L., Prospathopoulos, A. and Papadopoulos, A. 2001. Performance of three numerical wave models on the Aegean Sea. First results. *11th International Offshore and Polar Engineering Conference,* Vol. III, pp. 40-45. Stavanger, Norway.

Soukissian, T. & Theochari, Z. 2001. Joint occurrence of sea states and associated durations. *11th International Offshore and Polar Engineering Conference*, Vol. III, pp. 33-39. Stavanger, Norway.